



Thermoelectric properties of nanoporous three-dimensional graphene networks

Pradheep Thiyagarajan, Min-Wook Oh, Jong-Chul Yoon, and Ji-Hyun Jang

Citation: [Applied Physics Letters](#) **105**, 033905 (2014); doi: 10.1063/1.4883892

View online: <http://dx.doi.org/10.1063/1.4883892>

View Table of Contents: <http://scitation.aip.org/content/aip/journal/apl/105/3?ver=pdfcov>

Published by the [AIP Publishing](#)

Articles you may be interested in

[Enhanced thermoelectric performance of \(Ba,In\) double-filled skutterudites via randomly arranged micropores](#)
Appl. Phys. Lett. **104**, 142104 (2014); 10.1063/1.4870003

[Computational modeling and analysis of thermoelectric properties of nanoporous silicon](#)
J. Appl. Phys. **115**, 124316 (2014); 10.1063/1.4869734

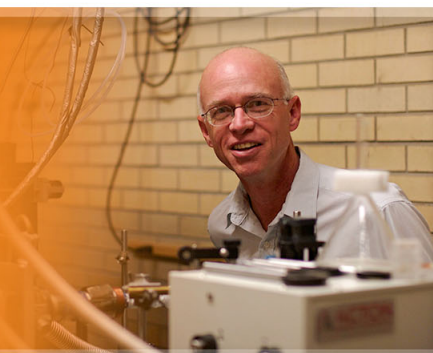
[Microstructure and thermoelectric properties of bulk and porous n-type silicon-germanium alloy prepared by HUP](#)
AIP Conf. Proc. **1449**, 409 (2012); 10.1063/1.4731583

[Effects of nanoscale porosity on thermoelectric properties of SiGe](#)
J. Appl. Phys. **107**, 094308 (2010); 10.1063/1.3388076

[Thermoelectric properties of nanoporous Ge](#)
Appl. Phys. Lett. **95**, 013106 (2009); 10.1063/1.3159813

The logo for Applied Physics Letters (AIP) features the letters 'AIP' in a large, white, sans-serif font on the left. To its right is a vertical orange bar, followed by the words 'Applied Physics Letters' in a smaller, white, sans-serif font. The background of the logo is a dark orange with a subtle, abstract pattern of light-colored, curved lines.

is pleased to announce **Reuben Collins**
as its new Editor-in-Chief



Thermoelectric properties of nanoporous three-dimensional graphene networks

Pradheep Thiyagarajan,¹ Min-Wook Oh,² Jong-Chul Yoon,¹ and Ji-Hyun Jang^{1,a)}

¹Interdisciplinary School of Green Energy and Low Dimensional Carbon Materials Center, UNIST, Ulsan 689-798, South Korea

²Creative Electrotechnology Research Center, Korea Electrotechnology Research Institute, Changwon, South Korea

(Received 31 March 2014; accepted 5 June 2014; published online 23 July 2014)

We propose three dimensional-graphene nanonetworks (3D-GN) with pores in the range of 10 ~ 20 nm as a potential candidate for thermoelectric materials. The 3D-GN has a low thermal conductivity of 0.90 W/mK @ 773 K and a maximum electrical conductivity of 6660 S/m @ 773 K. Our results suggest a straightforward way to individually control two interdependent parameters, σ and κ , in the nanoporous graphene structures to ultimately improve the figure of merit value. © 2014 AIP Publishing LLC. [<http://dx.doi.org/10.1063/1.4883892>]

The energy-conversion efficiency of a thermoelectric material is evaluated by a dimensionless figure of merit (ZT), defined as $ZT = S^2\sigma T/\kappa$, where S is the Seebeck coefficient, σ is the electrical conductivity, κ is the thermal conductivity, and T is the temperature.¹ To be competitive with conventional refrigerators or power generators, thermoelectric materials with a ZT value greater than 3 are highly desirable.² The key problem in increasing ZT lies in the conflicting interdependence between the Seebeck coefficient, the electrical conductivity (which should be high) and the thermal conductivity (which should be low).³ The thermal conductivity can be written as $\kappa = \kappa_{ph} + \kappa_{el}$, where κ_{ph} is the lattice thermal conductivity and κ_{el} is the electronic thermal conductivity. κ_{el} can be varied by doping the materials,⁴ whereas κ_{ph} cannot be reduced below a critical limit without distorting the lattice structure.⁵ In general, κ_{ph} is greater than κ_{el} for most thermoelectric materials. The various approaches to reducing κ_{ph} include but are not limited to (i) changing the dimensionality of structures,⁶ (ii) making composite materials,⁷ or (iii) using porous materials.^{8,9} Out of the different approaches, porous structures seem to be a more viable option because the degree of reduction in the thermal conductivity is higher than the reduction of electrical conductivity by an order of magnitude. For example, Yang *et al.* reported the reduction of thermal conductivity by 2 orders of magnitude in nanoporous silicon structures with holes of different pitch sizes (55 nm, 140 nm, 350 nm) while preserving sufficient electrical conductivity. Synder and co-workers have extended the concept to mesoporous Bi₂Te₃ which shows a nearly 50% reduction (1.2 W/mK @ 300 K) in thermal conductivity compared to non-porous samples (2.4 W/mK @ 300 K).³ However, most of the telluride based thermoelectric materials are toxic and hazardous to the environment. Recent report validates the possibility of nanoporous graphene/carbon to a wide variety of applications.^{10,11}

Recent reports on theoretical studies of 2D-graphene antidot lattices (GAL) illustrate very low thermal conductivity values accompanied by one order reduction in electrical

conductivity values; but not many experiments have been reported on GAL.¹² Shi *et al.* reported that macroscopic graphene-based foam (MGF) with a pore diameter of around 500 μ m has low thermal conductivity, due to the randomly dispersed pores.¹³ However, there is more room to improve the ZT value in this structure. Based on findings by Yang, a major reduction in the thermal conductivity can be attained when pore size is smaller than the phonon mean free path (MFP). The phonon MFP of graphene at room temperature is \sim 775 nm,¹⁴ so nanometer sized pores could cause a more effective drop in the thermal conductivity values than micron sized pores. We hypothesized that by introducing pores with a diameter of 10 ~ 20 nm into graphene, the thermal conductivity could be greatly reduced to a large extent while maintaining a reasonable electrical conductivity.

The detailed synthesis procedure of nanoporous three-dimensional graphene networks (3D-GN) is described elsewhere.¹⁵ Briefly, \sim 20 nm silica particles were coated with poly vinyl alcohol/iron chloride solution and carbonized at 1000 °C for 30 min under inert conditions. The silica particles and the residue materials were removed by means of chemical etching leaving behind porous graphene powders. The powders were dried at 90 °C for 3 h and used for further characterizations (Refer to supplementary material¹⁶ for more details).

Fig. 1(a) shows TEM images of the 3D-GN with pores around 10–20 nm; pores are highlighted in orange color. The pore size agrees well with that of the silica particles used for synthesis. The inset is a large area SEM image of 3D-GN

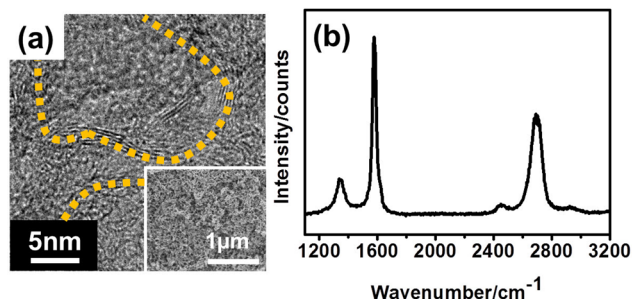


FIG. 1. (a) TEM image of 3D-GN highlighting pores in orange colour. The inset shows a large area SEM image of 3D-GN, (b) Raman spectrum of 3D-GN.

^{a)}Author to whom correspondence should be addressed. Electronic mail: clau@unist.ac.kr

showing uniform distribution of the pores (see Figure S3 in supplementary material). Fig. 1(b) shows the Raman spectrum of the synthesized 3D-GN powder. The spectrum indicates low defects in the samples, which is also reflected by a good I_D/I_G ratio. The integrated height method was used to calculate the ratio of Raman peaks, and the I_D/I_G and I_{2D}/I_G ratios were found to be 0.15 and 0.63, respectively, which proves the crystallinity of the sample. The intensity of the 2D peak shows the graphene has few to many layers.

Fig. 2(a) indicates the electrical conductivity of 3D-GN measured over a temperature range of 298–773 K. The pellets used for the measurements were consolidated at 1273 K under a pressure of 50 MPa for a holding time of 5 min using a spark plasma sintering system (Dr. Sinter, SPS-systex, Japan). The electrical conductivity of the material is given by

$$\sigma = ne\mu, \quad (1)$$

where n is carrier concentration, e is the electronic charge, and μ is the mobility. The electrical conductivity increases with temperature from 5210 S/m at 298 K to 6660 S/m at 773 K, indicating the appearance of semiconductor nature of 3D-GN. This can be attributed to the distortion of sp^2 lattice caused by the presence of pores, which causes the behaviour of 3D-GN to change from a semi-metal to a semiconductor. In GAL structure, the bandgap opening depends on the dimension of the holes as well as the wall distance between the holes.¹⁷ The bandgap opening makes a nonzero effective mass which considerably degrades carrier mobility, resulting in an inverse relation with mobility in the graphene nanoribbon structures.¹⁸ The electrical conductivity values in

3D-GN are higher than the previously reported values for nanoporous carbon¹⁹ (3030 S/m). Using Hall Effect measurement, the carrier concentration of 3D-GN was evaluated using $n = 1/eR_H$, where R_H is the Hall coefficient. The value of n for 3D-GN was $1.21 \times 10^{19} \text{ cm}^{-3}$ at room temperature.

Fig. 2(b) shows the thermal conductivity of 3D-GN measured using a laser flash apparatus (LFA 457) over temperature range. The thermal conductivity of the material can be calculated using

$$\kappa = adc, \quad (2)$$

where a is the thermal diffusivity, d is density, and c is the specific heat. The thermal conductivity values increases from 0.54–0.90 W/mK over temperature range of 298–773 K, due to electron-phonon nonequilibrium at high electron temperatures.²⁰ This can be explained using the Wiedemann-Franz law,²¹ $K_e = \sigma L T_e$, where σ is charge conductivity, L is the Lorenz number ($=2.45 \text{ E-}8 \text{ W}\Omega\text{K}^{-2}$),²² and T_e is the electronic temperature. In our samples, the contribution of phonons is dominant over the entire temperature range, as evidenced from electronic thermal conductivity values (Fig. 2(c), calculated from the Wiedemann-Franz law) which are much lower than phononic thermal conductivity values (Fig. 2(d)), thus confirming electron-phonon nonequilibrium in 3D-GN. The electron-phonon non equilibrium also exists in nanoporous gold structures²⁰ and GAL structures²³ reported earlier. Importantly, the 3D-GN showed greatly reduced thermal conductivity values than the few layer graphene (FLG) (1300–2700 W/mK) as will be described in Fig. 3. The κ value of FLG can be varied depending on any one or a combination of the following processes: boundary scattering, charged

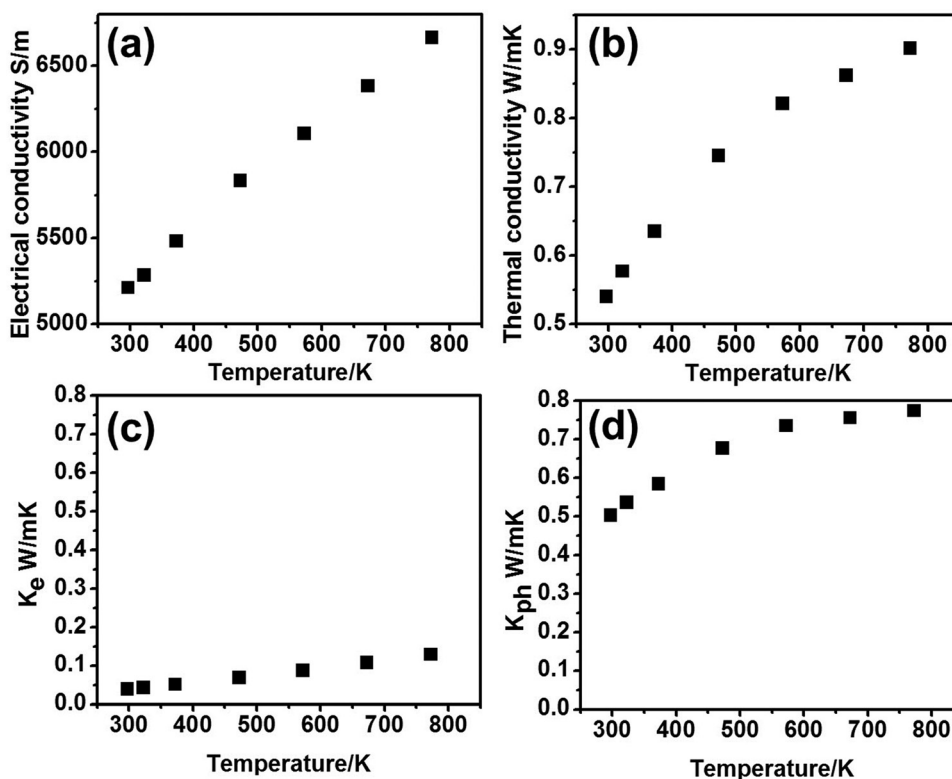


FIG. 2. (a) Electrical conductivity of 3D-GN, (b) the total thermal conductivity of 3D-GN, (c) the electronic thermal conductivity and (d) the phononic thermal conductivity of 3D-GN.

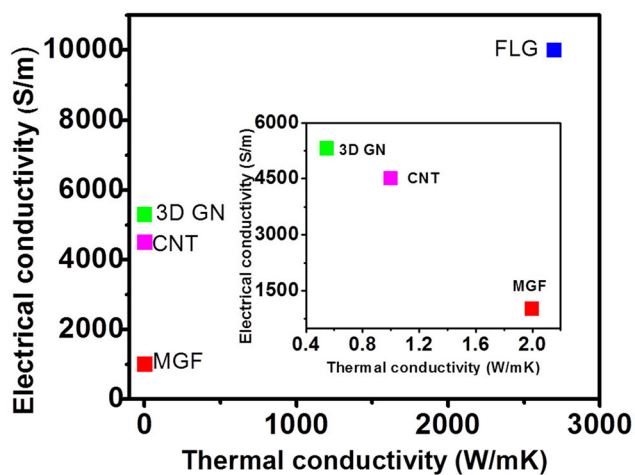


FIG. 3. Electrical conductivity and the thermal conductivity of carbon-based materials. The inset shows the low thermal conductivity region.

impurity scattering, and Umklapp process. In FLG samples, the scattering from the surface (top & back) of the graphene and charged impurity scattering of the graphene are minimal whereas the major reduction in thermal conductivity is governed by the Umklapp process.²⁴ The reduction in κ value of 3D-GN due to pores might cause a reduction in phonon group velocities and flattening of the phonon band, which causes change in Umklapp process. This large difference in the κ value is also due to the numerous interfaces of the 3D-GN, which interrupt phonon transport. In addition, the 3D-GN can be assumed to be a partly phononic crystal, wherein the pores act as channels of air between carbon atoms, which also contributes to the low κ value. The necking effect which was observed as a major cause of the reduction in thermal conductivity values of other porous materials such as nanoporous Si,²⁵ nanoporous Ge,⁹ etc. was also present in our material.

The thermoelectric properties of 3D-GN measured at room temperature were compared with previously reported data of other carbon-based thermoelectric materials as shown in Fig. 3 and Table I. We confirmed much enhanced performances of our 3D-GN compared to those of others. First, 3D-GN presents a much reduced thermal conductivity but a somewhat lower electrical conductivity than those of FLG. Since our structure resembles a GAL structure, the σ is inevitably lower than FLG, and this may be attributed to (i) opening of the electronic band gap due to pores and (ii) the dangling oxygen bonds around holes, which cannot be eliminated in our experimental constraints.²⁸ Second, differences in the structures which control heat transport properties were observed between 3D-GN and MGF. The thermal conductivity of 3D-GN is 4 times lower than that of MGF

TABLE I. Comparison of thermoelectric properties of the carbon-based materials measured at 300 K.

Carbon-Based Materials	Thermal conductivity (W/mK)	Electrical conductivity (S/m)
FLG ^{24,26}	1300–2700	10^4 – 10^5
3D-MGF ¹³	2.0	$\sim 10^3$
CNT ²⁷	1.0	4.5×10^3
3D-GN (in this study)	0.54	$\sim 5.2 \times 10^3$

whereas electrical conductivity is higher than MGF structures, implying much improved thermoelectric properties of 3D-GN to MGF. This is because the pore size and distance between walls in 3D-GN are in the nm range, whereas they are in the order of μm in MGF structures. Third, the degrees of the increase in σ and decrease in κ of the 3D-GN are slightly superior to very recently reported data from carbon nanotube (CNT). The decrease in thermal conductivity values in 3D-GN is attributed to the nm-size-hole porosity and roughness, both of which increase heat resistance by acting as centres for phonon scattering, which interrupts phonon transport through the structure, as we had hypothesized. Even though the electrical conductivity of the 3D-GN is found to be lower than FLG, it is comparatively higher than the values for CNT and MGF and can further be further improved by doping. Importantly, the contrast in values between the thermal and electrical conductivities suggests the possibility of increasing the σ -to- κ ratio through nanoporous structures.

In conclusion, we have studied the effects of nanometer-sized-holes in graphene over a wide temperature range, and illustrated the possibility of high ZT value in topological insulators of nanoporous three dimensional structures. The results suggest that the thermoelectric performance of nanoporous graphene is better at high temperatures (>600 K) than in the low temperature region (<400 K). Our result validates the hypothesis that two interdependent parameters, σ and κ , can be individually controlled in the nanoporous graphene structures to ultimately enhance the ZT value.

This work was supported by the Startup Research Fund (1.090040.01) of UNIST, by the NRF with the Contract No. NRF-2010-0019408, and by the Pioneer Research Center Program through the National Research Foundation of Korea funded by the Ministry of Science, ICT & Future Planning (No. NRF-2012-0001263).

¹A. F. Ioffe, *Semiconductor Thermoelements, and Thermoelectric Cooling* (Revised and supplemented for the English ed.) (Infosearch, London, 1957).

²G. G. Yadav, J. A. Susoreny, G. Q. Zhang, H. R. Yang, and Y. Wu, *Nanoscale* **3**(9), 3555–3562 (2011).

³Y. C. Zhang, T. Day, M. L. Snedaker, H. Wang, S. Kramer, C. S. Birkel, X. L. Ji, D. Y. Liu, G. J. Snyder, and G. D. Stucky, *Adv. Mater.* **24**(37), 5065–5070 (2012).

⁴G. Zhang and B. W. Li, *Nanoscale* **2**(7), 1058–1068 (2010).

⁵D. M. Rowe and V. S. Shukla, *J. Appl. Phys.* **52**(12), 7421–7426 (1981).

⁶M. S. Dresselhaus, G. Chen, M. Y. Tang, R. G. Yang, H. Lee, D. Z. Wang, Z. F. Ren, J. P. Fleurial, and P. Gogna, *Adv. Mater.* **19**(8), 1043–1053 (2007).

⁷M. Zebbarjadi, K. Esfarjani, M. S. Dresselhaus, Z. F. Ren, and G. Chen, *Energy Environ. Sci.* **5**(1), 5147–5162 (2012).

⁸D. W. Song, W. N. Shen, B. Dunn, C. D. Moore, M. S. Goorsky, T. Radetic, R. Gronsky, and G. Chen, *Appl. Phys. Lett.* **84**(11), 1883–1885 (2004).

⁹J. H. Lee and J. C. Grossman, *Appl. Phys. Lett.* **95**(1), 013106 (2009).

¹⁰Z. S. Wu, Y. Sun, Y. Z. Tan, S. B. Yang, X. L. Feng, and K. Mullen, *J. Am. Chem. Soc.* **134**(48), 19532–19535 (2012).

¹¹X. H. Li and M. Antonietti, *Angew. Chem. Int. Ed.* **52**(17), 4572–4576 (2013).

¹²T. Gunst, T. Markussen, A. P. Jauho, and M. Brandbyge, *Phys. Rev. B* **84**(15), 155449 (2011).

¹³M. T. Pettes, H. X. Ji, R. S. Ruoff, and L. Shi, *Nano Lett.* **12**(6), 2959–2964 (2012).

¹⁴D. L. Nika, E. P. Pokatilov, and A. A. Balandin, *Phys. Status Solidi B* **248**(11), 2609–2614 (2011).

- ¹⁵J. C. Yoon, J. S. Lee, S. I. Kim, K. H. Kim, and J. H. Jang, *Sci. Rep.* **3**, 1788 (2013).
- ¹⁶See supplementary material at <http://dx.doi.org/10.1063/1.4883892> for experimental details.
- ¹⁷F. P. Ouyang, S. L. Peng, Z. F. Liu, and Z. R. Liu, *Acs Nano* **5**(5), 4023–4030 (2011).
- ¹⁸J. Y. Wang, R. Q. Zhao, M. M. Yang, Z. F. Liu, and Z. R. Liu, *J. Chem. Phys.* **138**(8), 084701 (2013).
- ¹⁹V. V. Popov, S. K. Gordeev, A. V. Grechinskaya, and A. M. Danishevskii, *Phys. Solid State* **44**(4), 789–792 (2002).
- ²⁰P. E. Hopkins, P. M. Norris, L. M. Phinney, S. A. Policastro, and R. G. Kelly, *J. Nanomater.* **2008**, 418050.
- ²¹S. Yigen and A. R. Champagne, *Nano Lett.* **14**(1), 289–293 (2014).
- ²²H. S. Dow, M. W. Oh, B. S. Kim, S. D. Park, B. K. Min, H. W. Lee, and D. M. Wee, *J. Appl. Phys.* **108**(11), 113709 (2010).
- ²³V. M. Stojanovic, N. Vukmirovic, and C. Bruder, *Phys. Rev. B* **82**(16), 165410 (2010).
- ²⁴S. Ghosh, W. Z. Bao, D. L. Nika, S. Subrina, E. P. Pokatilov, C. N. Lau, and A. A. Balandin, *Nat. Mater.* **9**(7), 555–558 (2010).
- ²⁵J. Y. Tang, H. T. Wang, D. H. Lee, M. Fardy, Z. Y. Huo, T. P. Russell, and P. D. Yang, *Nano Lett.* **10**(10), 4279–4283 (2010).
- ²⁶N. Xiao, X. C. Dong, L. Song, D. Y. Liu, Y. Tay, S. X. Wu, L. J. Li, Y. Zhao, T. Yu, H. Zhang, W. Huang, H. H. Hng, P. M. Ajayan, and Q. Y. Yan, *Acs Nano* **5**(4), 2749–2755 (2011).
- ²⁷W. Y. Zhao, S. F. Fan, N. Xiao, D. Y. Liu, Y. Y. Tay, C. Yu, D. H. Sim, H. H. Hng, Q. C. Zhang, F. Boey, J. Ma, X. B. Zhao, H. Zhang, and Q. Y. Yan, *Energy Environ. Sci.* **5**(1), 5364–5369 (2012).
- ²⁸S. J. Yuan, R. Roldan, A. P. Jauho, and M. I. Katsnelson, *Phys. Rev. B* **87**(8), 085430 (2013).